Ultrasonics Sonochemistry 89 (2022) 106116

Contents lists available at ScienceDirect

Ultrasonics Sonochemistry

journal homepage: www.elsevier.com/locate/ultson

Multi-mode S-type ultrasound-assisted protein extraction from walnut dregs and *in situ* real-time process monitoring

Dandan Liu [a], Hongyan Di [a], Yiting Guo [a,b,*], Garba Betchem [a], Haile Ma [a,b,*]

[a] School of Food and Biological Engineering, Jiangsu University, 301 Xuefu Road, Zhenjiang, Jiangsu 212013, China
[b] Institute of Food Physical Processing, Jiangsu University, 301 Xuefu Road, Zhenjiang, Jiangsu 212013, China

ARTICLE INFO

Keywords:
Walnut dregs
Protein extraction
Multi-mode S-type ultrasound
Structural properties
Correlation
In situ real-time monitoring

ABSTRACT

This study aimed to investigate the impact of multi-mode S-type ultrasound treatment on the protein extraction level of walnut dregs. The structural properties of the walnut protein (WP) were characterized, and the correlation between protein structure and extraction level was analyzed. The *in situ* real-time monitoring model for the ultrasound-assisted WP extraction process was established by a miniature fiber near-infrared (NIR) spectrometer. Results showed that the protein yield, purity, and comprehensive extraction index (CEI) of extracted WP were 71.07 %, 72.69 %, and 71.72, respectively, under optimal conditions (dual-frequency 20/28 kHz, ultrasonic treatment duration 30 min, and ultrasound power density 120 W/L). The secondary structure of extracted WP displayed that the proportion of α-helix and β-sheet reduced, while the contents of β-turn and random coil increased after ultrasonic treatment. Besides, sonication decreased the disulfide bond content and increased free sulfhydryl (-SH) and surface hydrophobicity compared to the control. The microstructures of WP confirmed that appropriate sonication could unfold the protein aggregates and reduce the particle size. The extraction level of WP is positively correlated with the -SH content ($p < 0.01$). The quantitative prediction model of Si-PLS for -SH content in the ultrasound-assisted WP extraction process was established and performed a good correction and prediction performance ($Rc = 0.9736$; $RMSECV = 0.446$ μmol/L; $Rp = 0.9342$; $RMSEP = 0.807$ μmol/L). This study exploited a high-efficiency way for the WP extraction industry, and provided theoretical support for the development of the intelligent system in industrial protein extraction process.

1. Introduction

Walnut (*Juglans Regia* L.) is one of the most popular tree nuts worldwide due to its abundant nutritional elements and high economic value [1]. The cultivated area and production of walnut in China ranked first in the world for years [2]. An enormous number of walnuts are used for oil extraction, resulting in a large accumulation of walnut dregs [3]. As the main by-products of oil production, walnut dregs are rich in high-quality plant protein (>50 %) and generally used as forage, fertilizer, or even discarded, leading to a waste of resources and environmental pollution [4–6]. Protein extraction is considered an effective method to improve the comprehensive utilization and economic value of walnut dregs. As a conventional method to extract proteins, alkali-soluble extraction has been extensively applied in protein extraction due to its advantages of operational simplicity and cost-effectiveness [7]. However, alkali-soluble extraction has some shortfalls, including large solvent consumption, low extraction efficiency, and high energy consumption [8]. Moreover, alkali extraction may cause lysinoalanin formation, resulting in potential toxicity and lower nutritional value in resultant proteins [6,9]. Therefore, exploring a green, safe, and cost-effective protein extraction technique is paramount to satisfying the needs for high extraction efficiency and environmental protection.

Abbreviations: WP, walnut protein; NIR, near-infrared; CEI, comprehensive extraction index; -SH, sulfhydryl; S-S, disulfide bond; ANS, 8-Anilino-1-naphthalenesulfonic acid; DNTB, 5, 5′-dithio-bis-(2-nitrobenzoic acid); FT-IR, Fourier transform-infrared; SEM, scanning electron microscope; PLS, Partial least squares; iPLS, interval partial least squares; Si-PLS, synergy interval partial least square; *RMSECV*, root mean square error of cross-validation; *RMSEP*, root mean square error of prediction; *Rc*, correlation coefficient of the calibration set; *Rp*, correlation coefficient of the prediction set; SNV, standard normal variate transformation; SG, Savitzky–Golay smoothing; 1st Der, first derivative; 2nd Der, second derivative.

* Corresponding authors at: School of Food and Biological Engineering, Institute of Food Physical Processing, Jiangsu University, 301 Xuefu Road, Zhenjiang, Jiangsu 212013, China.

E-mail addresses: 1000005604@ujs.edu.cn (Y. Guo), mhl@ujs.edu.cn (H. Ma).

https://doi.org/10.1016/j.ultsonch.2022.106116
Received 29 May 2022; Received in revised form 26 July 2022; Accepted 4 August 2022
Available online 6 August 2022

As a green non-thermal physical processing technology, power ultrasound has been widely concerned and extensively applied in various food manufacturing [10,11]. At present, ultrasound-assisted extraction is regarded as an effective aid in the extraction of protein [6,12], oil [13], polyphenol [14], polysaccharides [15], and carotenoids [16], among others, due to its potent advantages of high extraction yield, less solvent consumption, lower maintenance costs, and environmental friendliness and sustainability [8]. Considerable amounts of recent studies have shown that ultrasonic-assisted protein extraction has potent attributes for improving yield and modifying the physical, structural, and functional properties of proteins [12,17,18]. This is mainly due to the combination of physical and chemical effects induced by acoustic cavitation that further enhance the mass transfer during the process [19]. However, conventional ultrasound-related works are carried out using probe- or bath-type ultrasound devices with a fixed frequency, which has some limits such as high intensity, small scale, and single working mode [20]. Our research group has been committed to developing multi-mode ultrasound equipment for many years and found that different ultrasonic working modes significantly influence the enhancement of protein extraction. The ideal working mode can significantly break the tightly bound protein molecules, changing the spatial structure and accelerating the protein dissolving. Therefore, a multi-mode S-type ultrasound device (Fig. 1) designed by our research group was applied in this study to extract walnut protein (WP), which could provide important technical support for the comprehensive development and utilization of walnut dregs.

Intelligent manufacturing is an inevitable trend in the development of the food industry in the future. Currently, the conventional methods for monitoring the key compounds in the extraction process rely on offline physicochemical detections, which cannot realize real-time dynamic monitoring. Near-infrared (NIR) spectroscopy has rapidly developed into a reliable analysis method in recent years due to the advantages of low cost, fast analysis, environmental protection, and online non-destructive testing [21,22]. NIR spectroscopy generally detects the molecular structural information of organic compounds containing hydrogen groups [23]. Due to the obvious differences in the wavelength and intensity of NIR absorption of different groups or the same group in different chemical environments, proteins with different secondary structure compositions give different NIR spectra, leading to the widespread application of NIR spectroscopy for monitoring structural changes in proteins [23,24]. Along with the development of miniature NIF fiber optic probe and its spectroscopic system, it can be conveniently placed into the extraction container for *in situ* real-time monitoring of protein structure. In this work, multi-mode ultrasound was applied in the WP extraction process to improve the protein extraction level. The yield, purity, and comprehensive extraction index (CEI) of WP were determined to evaluate the protein extraction level since an appropriate protein extraction process usually has the ability to increase protein yield and improve protein purity simultaneously. In addition, the effect of ultrasound-assisted extraction on the secondary structure, free sulfhydryl (-SH), disulfide bond (S—S), surface hydrophobicity, and microstructure of WP was studied. Correspondingly, the correlation between the extraction level and structural properties of WP was characterized by the Pearson correlation and stepwise multiple linear regression analyses. Finally, the *in situ* real-time monitoring model of NIF spectroscopy was established to improve the intellectualization of the WP extraction process.

2. Materials and methods

2.1. Materials

Walnut dregs were provided by Changbai Fairy Biotechnology Co., ltd. (Liaoning, China). 8-Anilino-1-naphthalenesulfonic acid (ANS) and 5, 5′-dithio-bis-(2-nitrobenzoic acid) (DNTB) were purchased from Sigma-Aldrich (St. Louis, MO, USA).

2.2. Ultrasound-assisted protein extraction from walnut dregs

The multi-mode S-type ultrasound device with five frequency generators (20, 28, 35, 40 and 52 kHz) was manufactured by Jiangsu University, which can achieve mono-, dual-, tri-, tetra- and penta- fixed frequency modes. The technological process of WP extraction assisted by the S-type ultrasound device is shown in Fig. 1. Ultrasound was applied continuously throughout the extraction process. In detail, the suspension of walnut dregs (40 g/L) was transferred to the sonication chamber

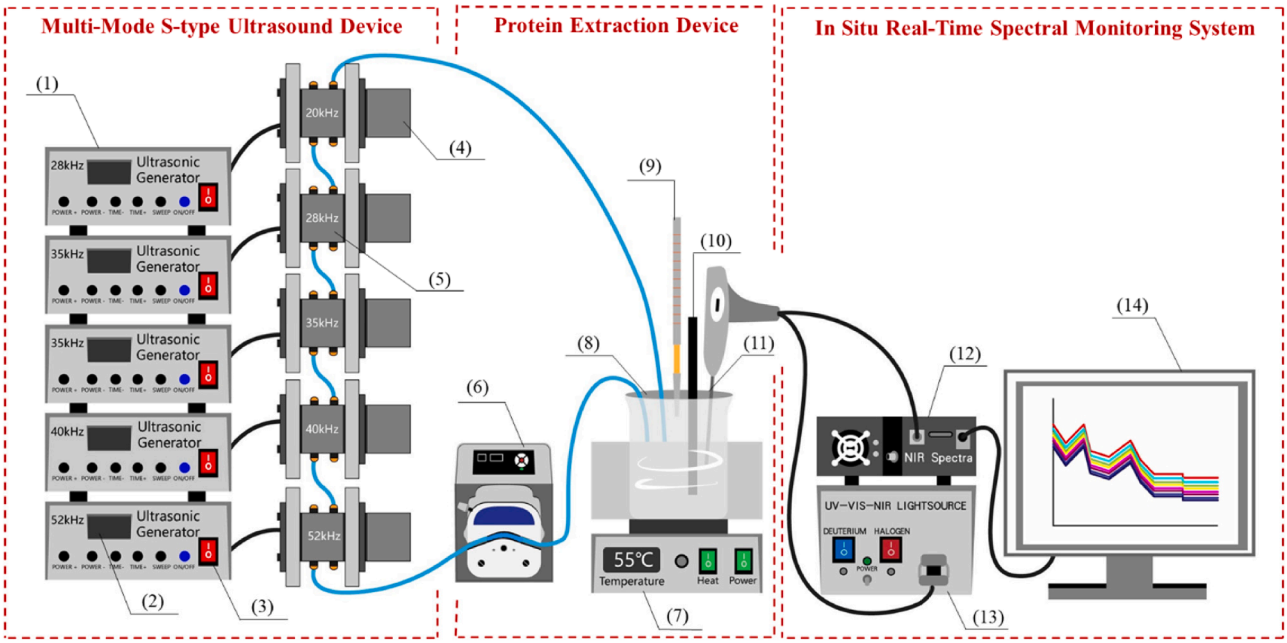

Fig. 1. The multi-mode S-type ultrasound device, protein extraction device, and *in situ* real-time spectral monitoring system. (1) ultrasonic generators; (2) viewing screen; (3) power supply; (4) ultrasonic transducer; (5) sonication chamber; (6) peristaltic pump; (7) Magnetic stirring water bath; (8) protein extraction container; (9) NaOH dropper; (10) pH electrode; (11) fiber optic probe; (12) near-infrared spectroscopy; (13) light source; (14) displayer.

by a peristaltic pump after stirring in a 50 °C water bath for 10 min. The pH of the whole extraction process was maintained at 9.0 with 1.0 M NaOH. The acoustic energy densities were set to 40, 60, 80, 100, 120, 140, and 120 W/L with the treatment durations of 10, 15, 20, 25, 30, 35, 40, 50, and 60 min under the different ultrasonic working modes. The supernatant of the obtained extracting solution was centrifugally concentrated and freeze-dried for the following measurement.

2.3. Protein extraction level assay

Protein extraction level was evaluated by determining protein yield and purity and computing the CEI value of WP. The supernatant of the extracted WP was dried and weighed, and protein yield was calculated as the following formula:

$$\text{Protein yield } (\%) = \frac{\text{The mass of dry matter in the extract}}{\text{Walnut dregs weight}} \times 100 \quad (1)$$

Protein purity was measured by the Kjeldahl method according to the AOAC Method 978.04.

CEI was computed as the following formula with the weighting coefficient of yield and purity set as 0.6 and 0.4, respectively.

$$\text{CEI } (\%) = (\text{Yield} \times 0.6 + \text{Purity} \times 0.4) \times 100 \quad (2)$$

2.4. Structural analysis

2.4.1. Fourier Transform-Infrared (FT-IR) spectroscopy

The secondary structure of WP was characterized by an FT-IR spectrometer (Thermal Nicolet, Madison, WI, USA) according to the method of Ding et al. [25] with some modifications. In brief, 10 mg extracted WP was mixed with 100 mg dried potassium bromide powder. The mixture was homogenized in an agate mortar and was formed into a pellet with a thickness of 0.3 mm using the hydraulic press. Eight scans were performed for all samples at 4 cm^{-1} resolution at 400–4000 cm^{-1}. The obtained spectrograms were analyzed by OMNIC (Thermo Fisher Scientific Inc., Waltham, MA, USA) and Peakfit (SeaSolve Software Inc., Framingham, MA, USA) softwares. The secondary structure of WP was identified, and content was calculated according to relevant literature [26].

2.4.2. Free -SH and S—S contents

The free -SH and S—S contents followed the method described by Lian et al. [18] with slight modifications. Lyophilized WP sample (100 mg) was dissolved in 10 mL of Tris-Gly buffer (0.086 M Tris, 0.09 M glycine, 4 mM EDTA, pH 8.0), stirred for 30 min, and then centrifuged at 5000 rpm for 20 min. One milliliter of the supernatant was collected and mixed with 5 mL of 0.5 % (v/v) sodium dodecyl sulfate standard buffer (86 mmol/L Tris, 90 mmol/L Gly, 8 mol/L urea, pH 8.0) and 50 μL of Ellman's reagent (4 mg/mL DTNB dissolved in standard buffer), and allowed to stand at 30 ℃ for 30 min. The absorbance at 412 nm was measured by a spectrophotometer (Unic7200, Unocal Corporation, Shanghai, China). The control was set up using an equal volume of Ellman's reagent instead of the protein sample. Free -SH content was calculated as follows:

$$C - SH\ (\mu mol/g) = \frac{73.53 \times \Delta Abs412 \times D}{C} \quad (3)$$

where $\triangle Abs$ is the difference in absorbance at 412 nm between the sample and control, D is the dilution ratio, and C is the protein concentration (mg/mL).

Sequentially, the S—S contents were measured according to the method of Lian et al. [18]. The S—S content was computed as follows:

$$C_{SS}(\mu mol/g) = \frac{C_{SH'} - C_{SH}}{2} \quad (4)$$

where $C_{SH'}$ is the total -SH content (μmol/g), and C_{SH} is the free -SH content in solution (μmol/g).

2.4.3. Surface hydrophobicity

The surface hydrophobicity of WP was analyzed by the fluorescence spectrophotometer (Cary Eclipse, Varian Inc., Palo Alto, USA) with the ANS as the probe method according to the study of Yang et al. [20]. The excitation and emission wavelengths were 240 nm and 450–550 nm, respectively, with a scanning speed of 120 nm/min and a slit size of 2.5 nm. The linear regression slope of fluorescence intensity to protein concentration is surface hydrophobicity.

2.4.4. Scanning electron microscope (SEM)

The microstructures of WP powder were photographed by an SEM (JSM-7001F, JEOL ltd, Tokyo, Japan) with an accelerating voltage of 15 kV. Before imaging, protein samples were mounted onto a specimen holder with the assistance of conductive tape and sputter-coated with gold. The micrographs were captured at 500 × magnifications.

2.5. In situ and real-time monitoring of WP extraction process by miniature NIR spectroscopy

The *in situ* real-time monitoring system of -SH content in WP extraction mainly includes a multi-mode S-type ultrasound device and a miniature NIR spectroscopy (NIRQUEST256-2.5, Ocean Optics, Largo, FL, USA) which is composed of a portable halogen light source (DH-2000-BAL, Ocean Optics), a fiber optical probe (TP300, Ocean Optics) with transmission and reflection modules, and a signal acquisition system (Fig. 1). Throughout the procedure of ultrasound-assisted WP extraction, the NIR probe remained immersed in the extracting solution to monitor the entire process.

During the ultrasound-assisted WP extraction process, an average of 3 sequential scans generated a NIR spectra every 2 min. The NIR spectrometer was operated with a scanning spectral region of 900–2500 nm. A total of 256 spectra with a resolution of 6.4 cm^{-1} were collected by using a 4 mm optical path transfer probe. Each original spectrum (Fig. 4b) was the average value of 3 scanning spectra. The background spectrum was collected before each NIR measurement using distilled water under the same experimental conditions. However, spectral data preprocessing is necessary before the model calibration stage due to the presence of unrelated information (such as baseline drift, background or instrumental noise). Meanwhile, the samples corresponding to each spectrum were collected to determine the -SH content.

2.6. Data analysis

2.6.1. Statistical analysis

Data were expressed as the mean ± standard deviation. The differences were evaluated using the one-way analysis of variance. Statistical analysis was accomplished using SPSS 19.0 (SPSS Inc., USA) software.

2.6.2. Correlation analysis

The correlation coefficient between protein structure changes and the extraction level of WP during the ultrasound-assisted extraction process was calculated by Pearson's correlation. Stepwise multiple linear regression was conducted to correlate the quantitative relationship between a dependent variable (protein yield) and multiple independent variables (α-helix, β-sheet, β-turn, random coil, surface hydrophobicity, -SH, and S—S content).

2.6.3. Multivariate analysis

The SPXY algorithm was used to divide the calibration set and prediction set spectrum, and the measured values and *in situ* spectra were divided into a calibration set with 64 samples and a prediction set with 16 samples (Supplementary Table S1). Partial least squares (PLS), interval partial least squares (iPLS), and synergy interval partial least square (Si-PLS) were used for wavelength interval screening to extract

representative information for modeling. The root mean square error of cross-validation (*RMSECV*), the root mean square error of prediction (*RMSEP*), the correlation coefficient of the calibration set (*Rc*), and the correlation coefficient of the prediction set (*Rp*) were adopted to evaluate the accuracy and stability of the respective model. Generally, models with high prediction ability performed the lower *RMSEC* and *RMSEP* values and higher *Rc* and *Rp* values. Additionally, models with high stability have less difference between *Rc* and *Rp* or *RMSECV* and *RMSEP* [27].

3. Results and discussion

3.1. Effects of ultrasound-assisted extraction on the extraction level of WP

In the process of ultrasound-assisted WP extraction, the protein yield, purity, and CEI value were used to evaluate the extraction level of WP. As depicted in Fig. 2a, ultrasound with different frequency modes remarkably affected the protein yield and CEI value, while no obvious effects were found on the protein purity. The extraction process assisted by the dual-frequency (20/28 kHz) achieved the highest protein yield (66.01 %), and CEI value (66.46) among tested frequency modes, followed by the mono-frequency of 28 kHz, while the lowest protein yield and CEI value were found at 52 kHz. The results indicate that multi-mode ultrasound treatment was an effective aid in improving the protein extraction level in the process of WP extraction. Similarly, Qu et al. [6] reported that 28 kHz was more conducive to extracting heat-labile proteins from walnut meal due to the relatively high solubility promoting effect, while a higher frequency of ultrasound was prone to induce protein aggregation.

Under the ultrasonic treatment with dual-frequency (20/28 kHz) and power density of 120 W/L, the effect of processing durations on the protein extraction level was demonstrated in Fig. 2b. With the extraction proceeding, the protein yield of WP maintained an upward trend, while the protein purity and CEI value manifested an upgrade first and then a downward trend, and the peak values (72.69 % and 71.72, respectively) were found at 30 min. This might be due to the fact that the cavitation effect of ultrasound increased with the prolongation of treatment time, which promoted the mass transfer between solvent and solute and thus accelerated the dissolution of WP under alkaline condition [6]. However, the strong thermal effect induced by longtime ultrasonic treatment leads to protein decomposition, denaturation, and molecular aggregation, decreasing the extraction rate [28]. Our previous work extracted WP by the conventional alkali-soluble process without ultrasound, and the highest protein yield, purity, and CEI value were 66.16 %, 69.37 %, and 67.44, respectively, under the optimal extraction conditions (55 ℃, pH 9.0, and 60 min) [29]. Therefore, it is obvious that power ultrasound could not only shorten the extraction time greatly but also increase the protein yield, purity, and CEI value by 7.42 %, 4.79 %, and 6.35 %, respectively, which is conducive to saving production cost and reducing energy consumption.

Under the dual-frequency (20/28 kHz) and ultrasonic treatment duration of 30 min, the effect of ultrasonic power densities on the protein extraction level was evaluated. It can be observed in Fig. 2c that the protein yield, purity, and CEI value of WP increased significantly as the ultrasonic power density increased, reaching the maximum values of 71.07 %, 72.69 %, and 71.72 at 120 W/L, respectively, and then decreased. Literature has shown that higher power density could enhance the cavitation and mass transfer efficiency, which may lead to the destruction of secondary bonds that maintain the spatial structure of proteins, resulting in a looser structure of WP [30]. Taken together, the frequency, time, and power density of sonication all significantly influenced the protein extraction level in the WP extraction process. Therefore, to further explore the underlying mechanism of ultrasound treatment parameters to improve the protein extraction level, it is necessary to characterize the structural properties of WP during ultrasound-assisted extraction and study the correlation between protein structure and extraction level.

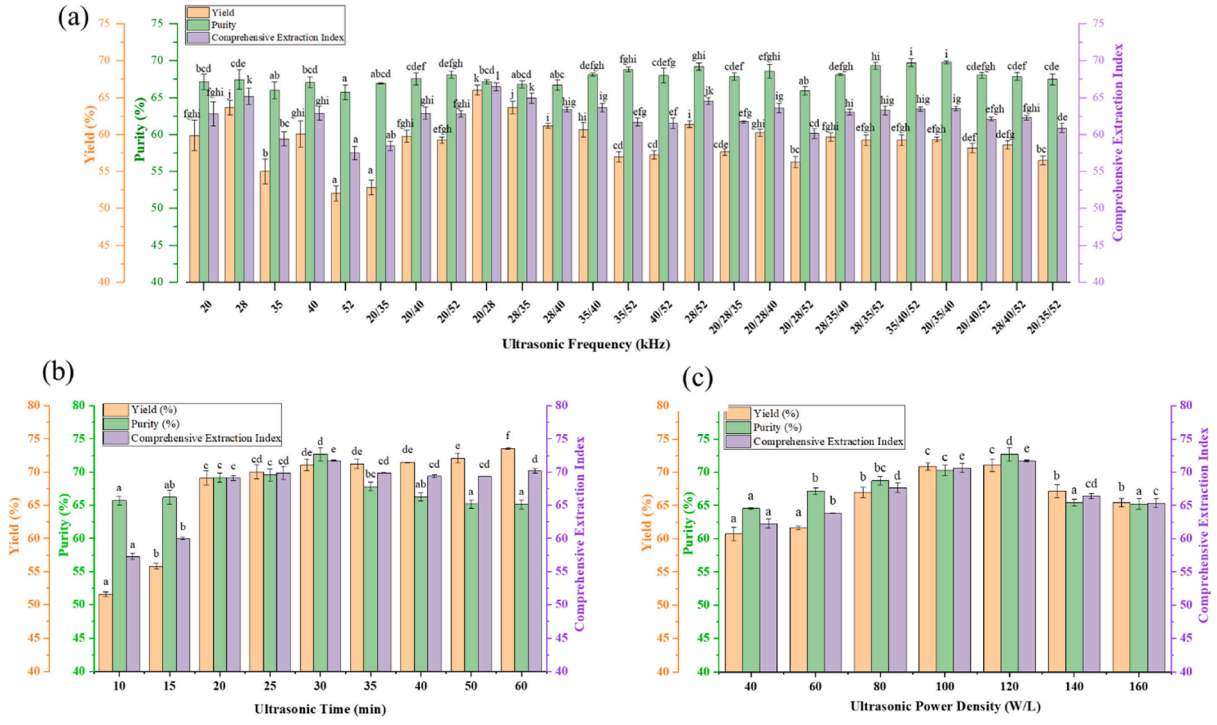

Fig. 2. Effects of ultrasonic frequencies (a), durations (b), and power densities (c) on the extraction level (protein yield, purity, and comprehensive extraction index) of walnut protein. Bars with different letters are significantly different ($p < 0.05$).

3.2. Effects of ultrasonic-assisted extraction on structural characteristics of WP

3.2.1. FT-IR analysis

The secondary structure of WP extracted using the ultrasound-assisted alkali method was characterized by analyzing the amide I region (1600–1700 cm^{-1}) FT-IR spectra. The relative contents of α-helix, β-turn, β-sheet, and random coil in WP are depicted in Table 1. In comparison with the control, the proportion of α-helix after ultrasonic treatment showed a downward trend except for the treatment time of 60 min, especially the treatment time of 15 min ($p < 0.01$) and 40 min ($p < 0.05$) and the ultrasonic power density of 100 and 160 W/L ($p < 0.01$). Similarly, the content of β-sheet in the samples treated with different ultrasonic times (20, 25, 30, 40, 60 min) and power density (100–160 W/L) decreased significantly ($p < 0.01$). Conversely, the proportion of β-turn and random coil increased significantly ($p < 0.01$) under the different ultrasound times and power densities. Literature has indicated that the α-helix and β-sheet represent the order state of protein molecules, while the β-turn and random coil reflect the looseness of protein [6]. The hydrogen bonds that maintain the stability of WP structure were weakened, and the protein structure changed from ordered to disordered under proper ultrasonication. In addition, it is noteworthy that the ultrasonic time and power density showed striking influences on the secondary structure of WP, especially the ultrasonic power density ranged from 100 to 160 W/L, the contents of the four secondary structures changed significantly ($p < 0.01$). These results indicate that ultrasound treatment could cause reallocation in the secondary structure of WP. Similarly, Zhu et al. [31] also reported that increasing intensity and duration of sonication caused slight modifications of the secondary structure in WP, such as the reduction of α-helix content and increase in the β-sheet, β-turn, and random coil content.

3.2.2. Free -SH and S—S contents

The free -SH and S—S are important functional bonds that participate in the formation of rigid structure, which can stably support the network structure of WP and make protein molecules more orderly [32]. The contents of the free -SH and S—S in WP extracted by the ultrasound-assisted alkaline method are shown in Table 2. It can be observed that the increasing power density and duration of sonication caused a significant increase ($p < 0.01$) in the -SH content and a reduction in the S—S content in comparison with the control. Similar results were found in rice protein [33], milk protein [22], and watermelon seed protein [28], which were all processed by ultrasound treatment. The cause for these results might be as follows: i) the shear force generated by sonication promoted partial unfolding of WP, which leads to the exposure of free -SH groups originally existing in the hydrophobic interior of the protein molecule [34]; ii) the S—S bonds in the protein subunits were broken and converted to the free -SH under the sonication [18].

3.2.3. Surface hydrophobicity

Surface hydrophobicity is an important indicator for assessing the strength of non-covalent bonds on the surface of protein molecules. The surface hydrophobicity of WP treated by different ultrasonic parameters is shown in Table 2. With the prolongation of ultrasonic extraction duration, the surface hydrophobicity of WP fluctuated and reached the

Table 1
Effects of ultrasonic duration and power density on the secondary structure of walnut protein.

Ultrasonic treatment condition		α-helix (%)	β-turn (%)	β-sheet (%)	Random coil (%)
Control		18.64 ± 0.26	11.10 ± 0.11	56.47 ± 0.33	13.80 ± 0.04
Ultrasonic duration (min)	10	16.97 ± 0.04	12.25 ± 0.24**	55.16 ± 1.05	14.50 ± 1.65
	15	14.18 ± 0.02**	17.17 ± 0.09**	54.69 ± 0.16	14.20 ± 0.39
	20	16.79 ± 0.23	12.90 ± 0.49**	49.61 ± 0.08**	14.51 ± 0.60
	25	17.45 ± 0.14	12.88 ± 0.42**	52.09 ± 1.49**	15.96 ± 0.93*
	30	16.88 ± 1.15	13.10 ± 0.31**	50.69 ± 1.90**	15.75 ± 0.87*
	35	17.04 ± 0.02	12.68 ± 0.12**	54.05 ± 0.12	15.87 ± 0.51*
	40	16.71 ± 1.94*	12.77 ± 0.43**	47.35 ± 1.51**	15.49 ± 0.43
	50	17.43 ± 0.09	12.59 ± 0.17**	55.26 ± 2.37	15.63 ± 0.73*
	60	22.92 ± 0.73*	12.81 ± 0.61**	49.39 ± 1.02**	15.51 ± 0.57
Ultrasonic power density (W/L)	40	16.52 ± 0.53	12.49 ± 0.37*	55.79 ± 1.52	15.23 ± 1.07
	60	17.01 ± 1.64	12.02 ± 0.49	56.20 ± 1.78	14.98 ± 0.68
	80	17.16 ± 1.35	12.31 ± 0.79	51.24 ± 0.70**	15.31 ± 1.39
	100	14.40 ± 0.67**	18.53 ± 0.75**	46.93 ± 0.66**	19.97 ± 0.50**
	120	16.88 ± 1.15	13.10 ± 0.31**	50.69 ± 1.90**	15.75 ± 0.87*
	140	18.18 ± 0.14	14.17 ± 1.41**	46.67 ± 1.19**	19.79 ± 1.05**
	160	14.58 ± 0.82**	18.38 ± 0.52**	46.57 ± 0.49**	20.48 ± 0.09**

Note: Control refers to the walnut dregs. Results are given as means ± SD (n = 3). * Significant differences ($p < 0.05$) and ** significant differences ($p < 0.01$) versus the control.

Table 2
Effects of ultrasonic duration and power density on the -SH, S—S, and surface hydrophobicity.

Ultrasonic treatment condition		-SH (μmol/g)	S—S (μmol/g)	Surface Hydrophobicity
Control		6.18 ± 0.19	15.99 ± 0.34	63.32 ± 15.74
Ultrasonic duration (min)	10	7.68 ± 0.17**	14.06 ± 1.60*	134.26 ± 13.31**
	15	8.17 ± 0.14**	14.18 ± 0.40*	142.54 ± 16.89**
	20	8.59 ± 0.16**	8.57 ± 0.39**	79.52 ± 14.63
	25	8.08 ± 0.11**	13.56 ± 1.20**	86.27 ± 3.98
	30	8.85 ± 0.09**	8.42 ± 0.06**	220.86 ± 11.20**
	35	8.69 ± 0.28**	8.99 ± 0.91**	140.99 ± 7.78**
	40	9.82 ± 0.11**	10.84 ± 0.26**	150.03 ± 24.40**
	50	10.14 ± 0.35**	10.02 ± 0.39**	86.81 ± 12.89
	60	10.57 ± 0.05**	15.06 ± 0.06	66.56 ± 6.91
Ultrasonic power density (W/L)	40	8.70 ± 0.07**	11.08 ± 0.24**	72.05 ± 6.74
	60	8.04 ± 0.16**	12.84 ± 0.85**	76.70 ± 11.24
	80	8.36 ± 0.12**	14.81 ± 0.87	85.65 ± 13.64
	100	9.52 ± 0.06**	14.57 ± 0.55	199.15 ± 7.32**
	120	8.85 ± 0.09**	8.42 ± 0.06**	220.86 ± 11.20**
	140	10.20 ± 0.40**	13.73 ± 0.97*	236.31 ± 15.95**
	160	8.87 ± 0.17**	12.50 ± 1.39**	294.24 ± 38.33**

Note: Control refers to the walnut dregs; -SH, free sulfhydryl content; S—S, disulfide bond content. Results are given as means ± SD (n = 3). * Significant differences ($p < 0.05$) and ** significant differences ($p < 0.01$) versus the control.

maximum value (220.86 ± 11.20) at 30 min, and then gradually decreased. Hydrophobic groups and regions contained in the interior of protein molecules might be exposed under the suitable sonication, resulting in increased surface hydrophobicity of WP. Besides, the high pressures, temperatures and shear forces generated by ultrasound may break the chemical bonds that link proteins to other components, thereby loosening the protein tissue and increasing its surface hydrophobicity [35]. However, prolonged ultrasonic treatment duration could induce protein re-curling and partial exposed hydrophobic groups refolding to form aggregates, thus reducing the surface hydrophobicity [36]. This finding was consistent with the studies on the watermelon seed protein [28], rice protein [20], and milk protein [22]. In addition, the ultrasonic power density significantly affected the hydrophobicity value of WP. With the increase in power density (especially over 100 W/L), the surface hydrophobicity of WP increased significantly ($p < 0.01$) compared with the control, indicating that the effect of high-intensity ultrasound on the surface hydrophobicity of WP may be greater than the low-intensity ultrasound.

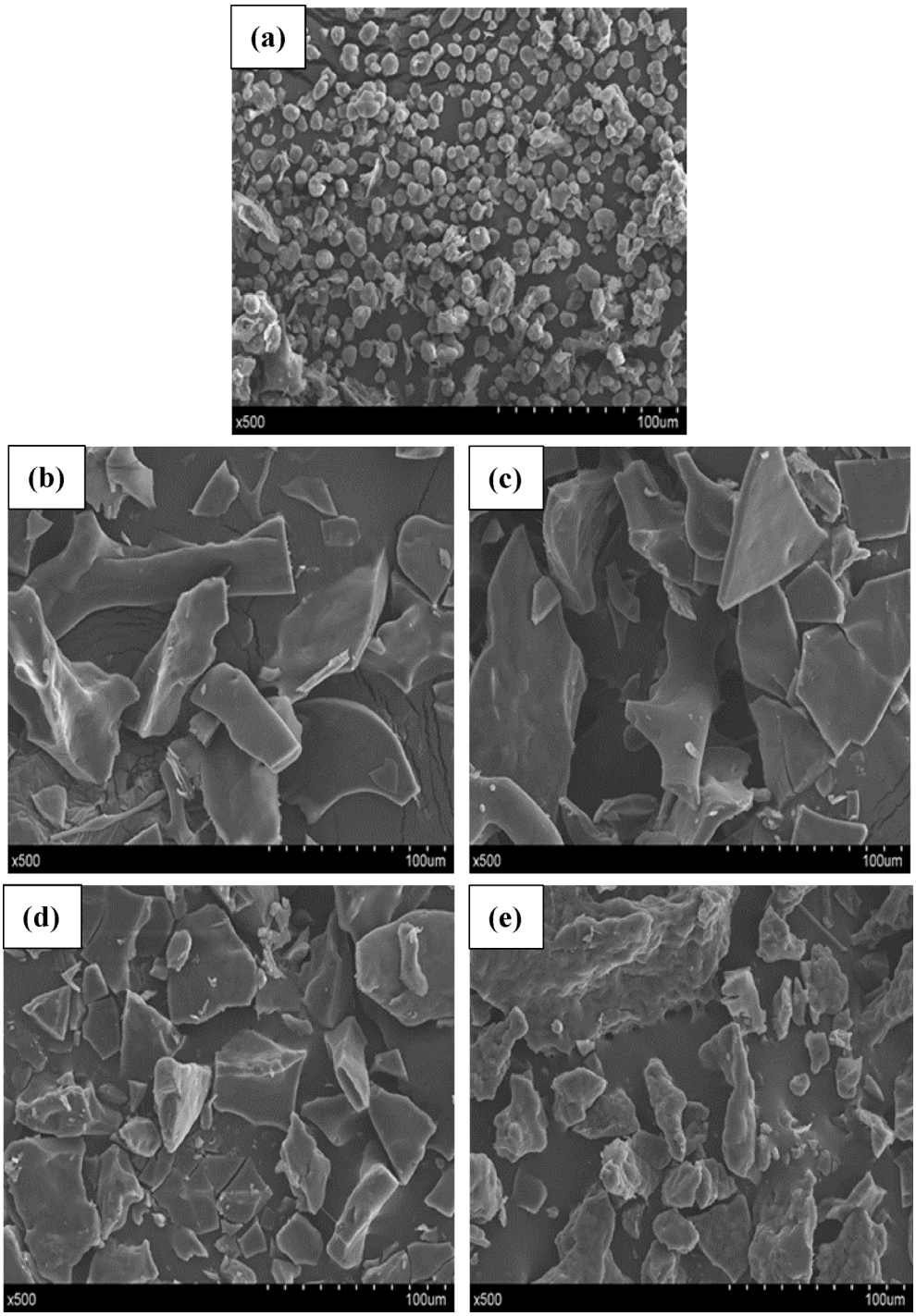

Fig. 3. Scanning electron micrograph (SEM) of walnut protein under different conditions. (a) control (walnut dregs); (b) walnut protein from alkali extraction (30 min); (c) walnut protein from alkali extraction (60 min); (d) walnut protein from ultrasound-assisted alkali extraction (30 min); (e) walnut protein from ultrasound-assisted alkali extraction (60 min).

3.2.4. Microstructure analysis

SEM analyzed the influence of ultrasound-assisted extraction on the microstructure of WP at the magnification of 500. As shown in Fig. 3, the control (walnut dregs) showed relatively regular spheroids (Fig. 3a), while the WP extracted by alkali or ultrasound-assisted alkali methods tended to form relatively thin, irregularly shaped sheets and present an incompact surface structure. These results indicated that the protein extraction process could change the WP microstructure and increase its specific surface area, which was conducive to improving the protein solubility. From Fig. 3b and Fig. 3d, the extracted WP assisted with ultrasound showed a smaller flaky plate shape at the same processing time compared with the single alkali extraction. A similar phenomenon was found in the research of Zhu et al. [31], who reported that the cavitation and turbulent force caused by sonication destroyed the protein break more thoroughly. However, the image of WP from ultrasound-assisted extraction for 60 min (Fig. 3e) showed larger sheets than 30 min treatment (Fig. 3d), suggesting the formation of larger aggregates. Resendiz-Vazquez et al. [37] reported that the possible reason for the protein molecule reaggregating was that ultrasound promoted protein unfolding and exposed the hydrophobic regions and free-SH, which could interact with each other and cause the formation of aggregates.

3.3. Correlation between protein structure and extraction level of WP

The correlation between extraction level (yield, purity, and CEI value) and the structural parameters (α-helix, β-sheet, β-turn, random coil, surface hydrophobicity, -SH and S—S content) of WP during the ultrasound-assisted protein extraction was explored by Pearson correlation coefficient, and the results are shown in Table 3. The correlation coefficient typically indicates how two variables correlate linearly [38]. The larger the absolute value of the correlation coefficient, the stronger the correlation. The correlation of -SH content with the protein yield and CEI value was significant ($p < 0.05$), especially the protein yield ($p < 0.01$), and the correlation coefficients were 0.641 and 0.503, respectively. The results suggest that the content of free -SH in extracting solution could reflect the extraction level of WP, and the high free -SH content could increase protein yield. This may be due to the breakdown of chemical bonds that maintain the network structure of the protein, resulting in high contents of free -SH and an increase in protein solubility as extraction progress.

Stepwise multiple linear regression analysis was applied to quantify the relationship between extraction level and protein structure of WP, and the results were shown in Figure S1. The regression equation is Y (protein yield) = 24.715 + 4.711 X_6 (-SH content). R^2 of the model was 0.966, indicating the model fitted the sample well. The F value was 9.764 and $p < 0.01$, suggesting that the regression equation was significant. The results indicated that the change of -SH content during ultrasound-assisted WP extraction was the main influence factor for the variation of protein yield and CEI value. Therefore, -SH content could be used to predict the protein yield of WP, thereby judging the endpoint of ultrasound-assisted WP extraction.

3.4. Establishment of in situ real-time monitoring model of the protein extraction process by NIR spectroscopy

The *in situ* real-time monitoring model for the ultrasound-assisted WP extraction was established by combining the NIR spectroscopy with the -SH content measured by off-line sampling during the protein extraction process. The variation of -SH content in the ultrasound-assisted WP extraction under the different ultrasonic power densities were shown in Fig. 4a, and its corresponding original NIR spectra were exhibited in Fig. 4b. As depicted in Fig. 4a, under the different power densities, the -SH content in the extracting solution of WP gradually increased as the extraction proceeded. The original NIR spectrum collected by the *in situ* real-time monitoring system contains some information unrelated to the changes in protein structure, such as background information, mechanical agitation, baseline drift and scattering of WP particles [22,39]. Therefore, pretreatment with stoichiometry is necessary to remove interference and useless information before the model calibration stage. In this work, the original spectrum was preprocessed *via* standard normal variate transformation (SNV), Savitzky–Golay smoothing (SG), first derivative (1st Der), and second derivative (2nd Der). PLS was used to establish the corresponding quantitative analysis model and determine the optimal pretreatment method. The preprocessed spectrum and the *RMSECV*, *RMSEP*, *Rp*, and *Rc* values are shown in Fig. 4c. It can be observed that SNV and SG preprocessing could enhance the spectral features and remove noise and background interference, while the spectrum preprocessed by 1st Der and 2nd Der amplified the irrelevant signal and noise and lost part of effective information. Moreover, the prediction model of the ultrasound-assisted WP extraction with SG preprocessing showed a better performance than other pretreatment methods, where *RMSECV* = 0.85, *RMSEP* = 0.996, *Rc* = 0.9064, and *Rp* = 0.8743. Therefore, spectral data based on SG preprocessing was chosen for further analysis.

PLS, iPLS, and Si-PLS were used to establish quantitative models for predicting the -SH content in the ultrasound-assisted WP extraction. The stability and accuracy of the models were analyzed by comparing *Rc*, *Rp*, *RMSECV*, and *RMSEP* values. As depicted in Fig. 5, the *Rc* and *Rp* (0.9393 and 0.9677, respectively) of the Si-PLS model were the highest, and the *RMSECV* and *RMSEP* (0.693 and 0.644, respectively) were the lowest among the three models, indicating that the stability and accuracy of the Si-PLS model were superior to the models established by PLS and iPLS in terms of the -SH content during the ultrasound-assisted WP extraction. Si-PLS divides the entire spectrum into several sub-intervals and then combines several sub-intervals for feature information screening, thereby eliminating redundant useless information and getting the utmost out of the useful information. Therefore, the entire spectrum was divided into 10–30 intervals, and 4 sub-intervals were combined for modeling. The optimal combined interval was selected by comparing the correlation coefficient (*Rc* and *Rp*) and root mean square error (*RMSECV* and *RMSEP*) values. The results of the Si-PLS model in different sub-intervals are displayed in Table 4. The highest *Rc* value (0.9736) and the lowest *RMSECV* value (0.446) were found when the spectrum was divided into 21 intervals with the principal components of

Table 3
Pearson correlation coefficient (*r*) and significance level (*P*-value) of walnut protein structure performance and extraction index.

Extraction index	α-helix (%)	β-sheet (%)	β-turn (%)	Random coil (%)	Surface hydrophobicity	-SH (μmol/g)	S—S (μmol/g)
r							
Yield	0.313	−0.458	−0.108	0.284	0.073	**0.641****	−0.362
Purity	0.01	−0.254	−0.098	−0.059	0.241	−0.246	−0.404
CEI	0.278	−0.465	−0.119	0.235	0.124	**0.503***	−0.418
P							
Yield	0.237	0.074	0.691	0.286	0.787	**0.007**	0.168
Purity	0.97	0.343	0.718	0.827	0.369	0.358	0.12
CEI	0.297	0.069	0.661	0.381	0.647	**0.047**	0.107

Note: CEI, comprehensive extraction index; -SH, free sulfhydryl content; S—S, disulfide bond content.

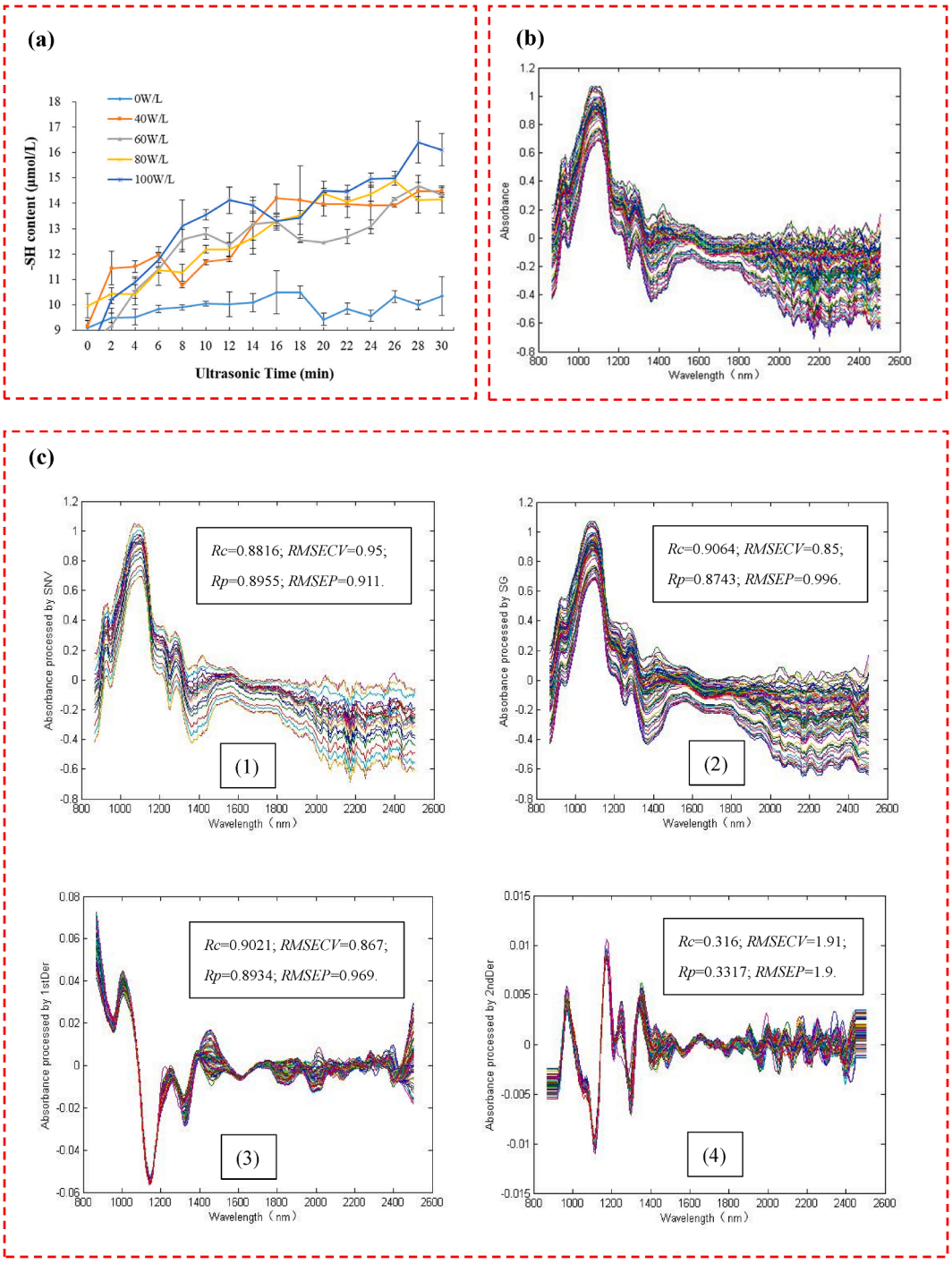

Fig. 4. (a) The change of -SH content during the ultrasound-assisted walnut protein extraction process; (b) Near-infrared original spectra of walnut protein during ultrasound-assisted extraction process; (c) Near-infrared spectrum preprocessed by different methods: (1) standard normal variate transformation (SNV); (2) Savitzky–Golay smoothing (SG); (3) first derivative (1st Der), and (4) second derivative (2nd Der).

9, suggesting that the Si-PLS model under the optimal combinations of intervals [2,4,9,15] was more relevant to the -SH content in the WP extraction process. The corresponding spectral ranges were 946.946–1018.601, 1103.101–1174.448, 1490.646–1561.283, and 1950.876–2020.772 nm (Fig. 6a). The 4 sub-intervals only account for 17.75 % of the entire spectral data, eliminating the influence of redundant data on the model, thus improving the calculation speed and performance of the model. Under the optimal combinations of intervals of the Si-PLS model, the quantitative model established for the -SH content in ultrasonic-assisted WP extraction is shown in Fig. 6b and c. In the calibration set, the *Rc* and the *RMSECV* were 0.9736 and 0.446 μmol/L, respectively, and the *Rp* and the *RMSEP* were 0.9342 and 0.807 μmol/L, respectively, in the prediction set. The Si-PLS model based on the NIR spectra and chemical value of -SH content of WP during ultrasound-assisted protein extraction had a good correction and prediction performance. The *in situ* and real-time monitoring system combined Si-PLS model can be applied to monitor WP structural changes in the ultrasound-assisted WP extraction process.

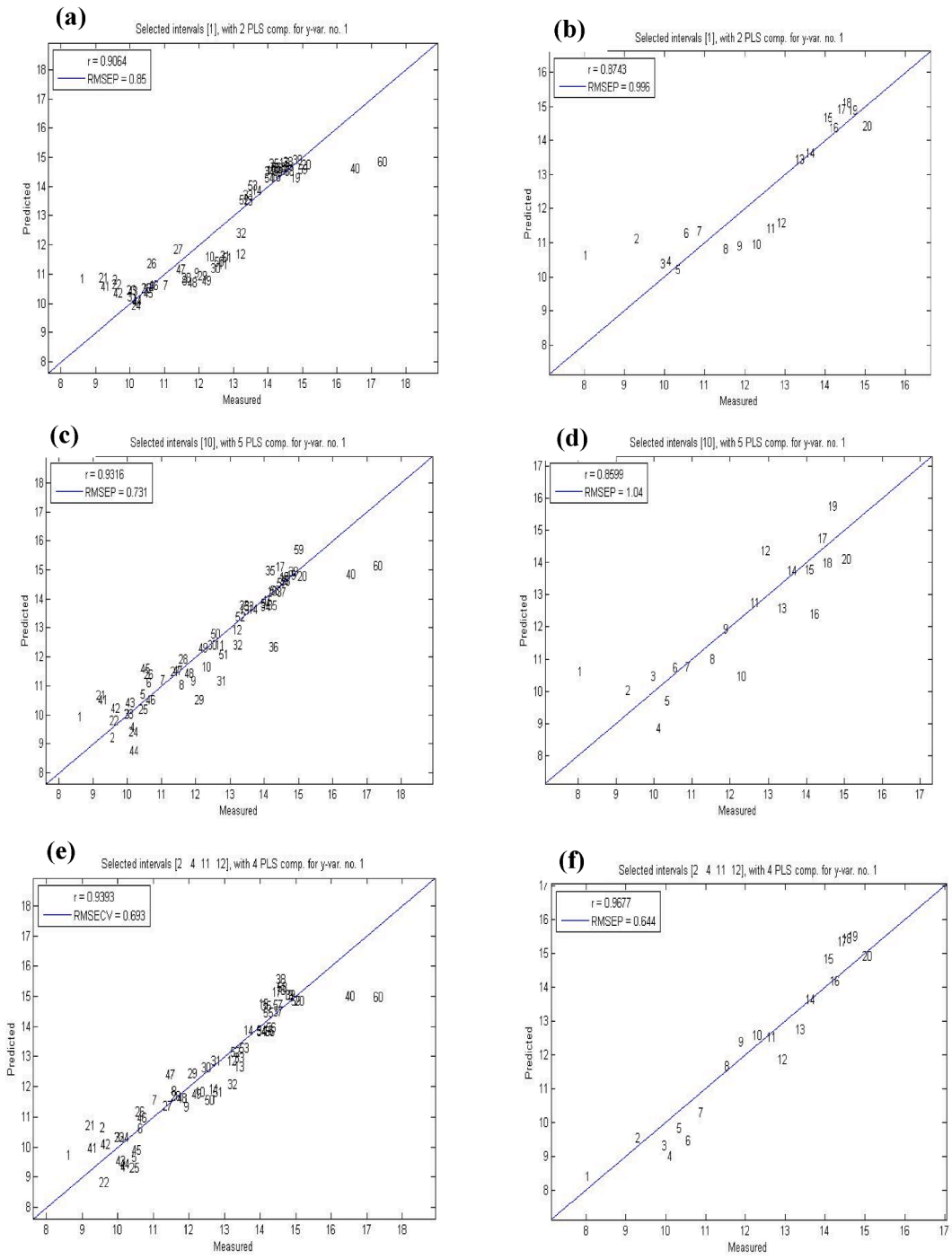

Fig. 5. Establishment of quantitative models of -SH content during the ultrasound-assisted walnut protein extraction process. (a) and (b): PLS calibration and predictive model; (c) and (d): iPLS calibration and predictive model; (e) and (f): Si-PLS calibration and predictive model.

4. Conclusions

Ultrasound-assisted protein extraction could be considered an effective way to improve the comprehensive utilization and economic value of walnut dregs. The protein yield, purity, and CEI value of WP increased remarkably under the appropriate ultrasonic treatment. In addition, sonication could cause protein structure changes, including the secondary structure reallocation, hydrophobic group exposure, and partial protein unfolding during the ultrasound-assisted WP extraction process. The results of correlation analysis demonstrate that -SH content was the main influence factor for the variation of WP extraction level. *In situ* and real-time monitoring model of the ultrasound-assisted WP extraction process was developed, which improved the efficiency of quality control and assurance of the protein extraction process.

CRediT authorship contribution statement

Dandan Liu: Conceptualization, Formal analysis, Writing – original draft. **Hongyan Di:** Methodology, Investigation. **Yiting Guo:** Writing – review & editing. **Garba Betchem:** Writing – review & editing. **Haile Ma:** Conceptualization, Resources, Supervision.

Table 4
Analysis results of Si-PLS model with -SH content under different sub-interval numbers.

Parameters	Number of subintervals	Selected subintervals	PCs	*Rc*	*RMSECV*	*Rp*	*RMSEP*
-SH content	10	[1,2,6,10]	7	0.9648	0.516	0.9442	0.801
	11	[2,5,6,8]	6	0.9695	0.48	0.9344	0.818
	12	[2,5,7,12]	9	0.9717	0.462	0.9313	0.874
	13	[2,6,7,10]	7	0.9661	0.510	0.9117	0.978
	14	[2,3,6,14]	10	0.9688	0.484	0.9313	0.852
	15	[2,3,8,11]	5	0.9667	0.499	0.9363	0.792
	16	[2,7,8,15]	9	0.9701	0.476	0.9117	0.926
	17	[2,3,7,15]	10	0.9651	0.514	0.9641	0.770
	18	[2,3,10,13]	8	0.9668	0.499	0.9427	0.746
	19	[2,3,8,17]	10	0.9718	0.460	0.9408	0.831
	20	[4,8,12,20]	10	0.9678	0.492	0.9439	0.891
	21	[2,4,9,15]	**9**	**0.9736**	**0.446**	**0.9342**	**0.807**
	22	[3,9,13,20]	10	0.9685	0.487	0.909	1
	23	[2,11,12,19]	10	0.9691	0.481	0.9562	0.687
	24	[3,7,10,21]	9	0.9593	0.483	0.9368	0.843
	25	[3,5,10,22]	10	0.9718	0.461	0.9411	0.809
	26	[3,5,11,23]	9	0.9708	0.469	0.9293	0.843
	27	[3,5,11,24]	9	0.9708	0.469	0.9293	0.843
	28	[3,5,12,25]	8	0.9707	0.469	0.9376	0.798
	29	[5,9,18,23]	10	0.9708	0.470	0.8982	1.070
	30	[4,9,18,24]	10	0.9731	0.451	0.9092	1.020

Note: PCs refer to principal components; *Rc* and *Rp* refer to the correlation coefficient of the calibration set and prediction set, respectively; *RMSECV* and *RMSEP* refer to the root mean square error of cross-validation and prediction, respectively.

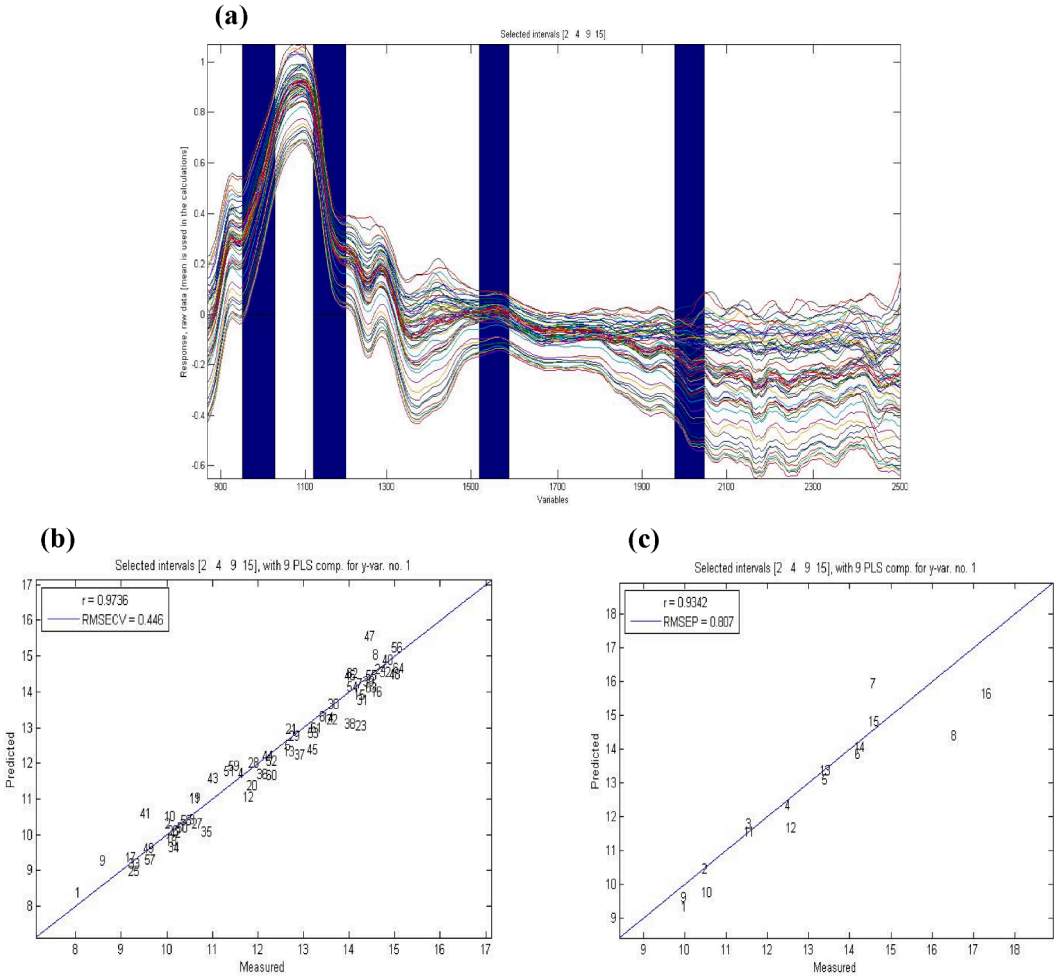

Fig. 6. The optimal sub-interval of the Si-PLS model (a), the scatter plot between measured and predicted values of Si-PLS model calibration set (b), and prediction set samples (c).

Declaration of Competing Interest

The authors declare that they have no known competing financial interests or personal relationships that could have appeared to influence the work reported in this paper.

Data availability

The authors do not have permission to share data.

Acknowledgments

The authors gratefully acknowledge the financial support provided by the National Programs for High Technology Research and Development of China grant (grant 2013AA102203) and the Key R&D Plan of Jiangsu Province (Key Project of Modern Agriculture) (BE2018368).

Appendix A. Supplementary data

Supplementary data to this article can be found online at https://doi.org/10.1016/j.ultsonch.2022.106116.

References

[1] C.J. Yan, Z. Zhou, Walnut pellicle phenolics greatly influence the extraction and structural properties of walnut protein isolates, Food Res. Int. 141 (2021), 110163, https://doi.org/10.1016/j.foodres.2021.110163.
[2] FAOSTAT, Food and Agriculture Organization. (Available at: http://www.fao.org/faostat/zh/#data/QC). (2021).
[3] Y.-X. Feng, Z.-C. Wang, J.-X. Chen, H.-R. Li, Y.-B. Wang, D.-F. Ren, J. Lu, Separation, identification, and molecular docking of tyrosinase inhibitory peptides from the hydrolysates of defatted walnut (*Juglans regia* L.) meal, Food Chem. 353 (2021) 129471.
[4] Q. Sun, Z.F. Ma, H.X. Zhang, S.J. Ma, L.M. Kong, Structural characteristics and functional properties of walnut glutelin as hydrolyzed: effect of enzymatic modification, Int. J. Food Prop. 22 (2019) 265–279, https://doi.org/10.1080/10942912.2019.1579738.
[5] X.Y. Mao, Y.F. Hua, Chemical composition, molecular weight distribution, secondary structure and effect of NaCl on functional properties of walnut (*Juglans regia* L) protein isolates and concentrates, J. Food Sci. Technol. Mysore 51 (2014) 1473–1482, https://doi.org/10.1007/s13197-012-0674-3.
[6] W. Qu, W. Fan, Y. Feng, Y. Li, H. Ma, Z. Pan, S. Cai, Preparation of heat-sensitivity proteins from walnut meal by sweep frequency ultrasound-assisted alkali extraction, J. Food Qual. 2021 (2021) 1–12, https://doi.org/10.1155/2021/9478133.
[7] M.K. Golly, H. Ma, D. Yuqing, L. Dandan, J. Quaisie, J.A. Tuli, B.K. Mintah, C. S. Dzah, P.D. Agordoh, Effect of multi-frequency countercurrent ultrasound treatment on extraction optimization, functional and structural properties of protein isolates from Walnut (*Juglans regia* L.) meal, J. Food Biochem. 44 (6) (2020).
[8] C.T. Wen, J.X. Zhang, H.H. Zhang, C.S. Dzah, M. Zandile, Y.Q. Duan, H.L. Ma, X. P. Luo, Advances in ultrasound assisted extraction of bioactive compounds from cash crops - A review, Ultrason. Sonochem. 48 (2018) 538–549.
[9] Y.H. Li, Z.L. Zhang, W.B. Ren, Y. Wang, B.K. Mintah, M. Dabbour, Y.Z. Hou, R. H. He, Y. Cheng, H.L. Ma, Inhibition Effect of Ultrasound on the Formation of Lysinoalanine in Rapeseed Protein Isolates during pH Shift Treatment, J. Agric. Food. Chem. 69 (2021) 8536–8545, https://doi.org/10.1021/acs.jafc.1c02422.
[10] K.-M. Song, S.K. Jung, Y.H. Kim, Y.E. Kim, N.H. Lee, Development of industrial ultrasound system for mass production of collagen and biochemical characteristics of extracted collagen, Food Bioprod. Process. 110 (2018) 96–103, https://doi.org/10.1016/j.fbp.2018.04.001.
[11] Y. Guo, B. Wu, D. Lu, Z. Pan, H. Ma, Tri-frequency ultrasound as pretreatment to infrared drying of carrots: impact on enzyme inactivation, color changes, nutrition quality parameters and microstructures, Int. J. Food Eng. 17 (2021) 275–284, https://doi.org/10.1515/ijfe-2020-0223.
[12] F. Wang, Y. Zhang, L. Xu, H. Ma, An efficient ultrasound-assisted extraction method of pea protein and its effect on protein functional properties and biological activities, LWT-Food Sci. Technol. 127 (2020), 109348, https://doi.org/10.1016/j.lwt.2020.109348.
[13] E. Riera, Y. Golas, A. Blanco, J.A. Gallego, M. Blasco, A. Mulet, Mass transfer enhancement in supercritical fluids extraction by means of power ultrasound, Ultrason. Sonochem. 11 (2004) 241–244, https://doi.org/10.1016/j.ultsonch.2004.01.019.
[14] C.S. Dzah, Y. Duan, H. Zhang, C. Wen, J. Zhang, G. Chen, H. Ma, The effects of ultrasound assisted extraction on yield, antioxidant, anticancer and antimicrobial activity of polyphenol extracts: A review, Food Biosci. 35 (2020), 100547, https://doi.org/10.1016/j.fbio.2020.100547.
[15] J. Zhang, C. Wen, W. Qin, P. Qin, H. Zhang, Y. Duan, Ultrasonic-enhanced subcritical water extraction of polysaccharides by two steps and its characterization from Lentinus edodes, Int. J. Biol. Macromol. 118 (2018) 2269–2277, https://doi.org/10.1016/j.ijbiomac.2018.07.098.
[16] Y. Li, A.S. Fabiano-Tixier, V. Tomao, G. Cravotto, F. Chemat, Green ultrasound-assisted extraction of carotenoids based on the bio-refinery concept using sunflower oil as an alternative solvent, Ultrason. Sonochem. 20 (2013) 12–18, https://doi.org/10.1016/j.ultsonch.2012.07.005.
[17] X.F. Ren, X. Wei, H.L. Ma, H.J. Zhou, J.J. Guo, S.Y. Mao, A. Hu, Effects of a dual-frequency frequency-sweeping ultrasound treatment on the properties and structure of the zein protein, Cereal Chem. 92 (2015) 193–197, https://doi.org/10.1094/cchem-03-14-0043-r.
[18] H. Lian, C. Wen, J. Zhang, Y. Feng, Y. Duan, J. Zhou, Y. He, H. Zhang, H. Ma, Effects of simultaneous dual-frequency divergent ultrasound-assisted extraction on the structure, thermal and antioxidant properties of protein from Chlorella pyrenoidosa, Algal Res. 56 (2021), 102294, https://doi.org/10.1016/j.algal.2021.102294.
[19] C. Wen, J. Zhang, H. Yao, J. Zhou, Y. Duan, H. Zhang, H. Ma, Advances in renewable plant-derived protein source: The structure, physicochemical properties affected by ultrasonication, Ultrason. Sonochem. 53 (2019) 83–98, https://doi.org/10.1016/j.ultsonch.2018.12.036.
[20] X. Yang, L. Wang, F. Zhang, H. Ma, Effects of multi-mode S-type ultrasound pretreatment on the preparation of ACE inhibitory peptide from rice protein, Food Chem. 331 (2020), 127216, https://doi.org/10.1016/j.foodchem.2020.127216.
[21] Y. Zhang, L. Luo, J. Li, S. Li, W. Qu, H. Ma, A.O. Oladejo, X. Ye, *In-situ* and real-time monitoring of enzymatic process of wheat gluten by miniature fiber NIR spectrometer, Food Res. Int. 99 (2017) 147–154, https://doi.org/10.1016/j.foodres.2017.03.048.
[22] P. Cui, X. Yang, Q. Liang, S. Huang, F. Lu, J. Owusu, X. Ren, H. Ma, Ultrasound-assisted preparation of ACE inhibitory peptide from milk protein and establishment of its *in-situ* real-time infrared monitoring model, Ultrason. Sonochem. 62 (2020), 104859, https://doi.org/10.1016/j.ultsonch.2019.104859.
[23] W. Wang, H. Jiang, G.-H. Liu, C.-L. Mei, Y. Ji, Qualitative prediction of yeast growth process based on near infrared spectroscopy, Chin. J. Anal. Chem. 45 (2017) 1137–1141, https://doi.org/10.1016/s1872-2040(17)61030-2.
[24] K. Izutsu, Y. Fujimaki, A. Kuwabara, Y. Hiyama, C. Yomota, N. Aoyagi, Near-infrared analysis of protein secondary structure in aqueous solutions and freeze-dried solids, Journal of Pharmaceutical, Science 95 (2006) 781–789, https://doi.org/10.1002/jps.20580.
[25] Y.H. Ding, H.L. Ma, K. Wang, S.M.R. Azam, Y.Y. Wang, J. Zhou, W.J. Qu, Ultrasound frequency effect on soybean protein: Acoustic field simulation, extraction rate and structure, LWT-Food Sci. Technol. 145 (2021), 111320, https://doi.org/10.1016/j.lwt.2021.111320.
[26] R. Khurana, A.L. Fink, Do Parallel β-Helix Proteins Have a Unique Fourier Transform Infrared Spectrum? Biophys. J. 78 (2000) 994–1000, https://doi.org/10.1016/S0006-3495(00)76657-4.
[27] K.S. Chia, H.A. Rahim, R.A. Rahim, Prediction of soluble solids content of pineapple *via* non-invasive low cost visible and shortwave near infrared spectroscopy and artificial neural network, Biosyst. Eng. 113 (2012) 158–165, https://doi.org/10.1016/j.biosystemseng.2012.07.003.
[28] C. Wen, J. Zhang, J. Zhou, Y. Feng, Y. Duan, H. Zhang, H. Ma, Slit divergent ultrasound pretreatment assisted watermelon seed protein enzymolysis and the antioxidant activity of its hydrolysates *in vitro* and *in vivo*, Food Chem. 328 (2020), 127135, https://doi.org/10.1016/j.foodchem.2020.127135.
[29] H. Di, H. Ma, Y. Wang, X. Ye, Y. Duan, Ultrasound-assisted extraction of the proteins from walnut meal, Modern, Food Sci. Technol. 35 (2019) 164–172, https://doi.org/10.13982/j.mfst.1673-9078.2019.7.023.
[30] S. Kangsanant, M. Murkovic, C. Thongraung, Antioxidant and nitric oxide inhibitory activities of tilapia (Oreochromis niloticus) protein hydrolysate: effect of ultrasonic pretreatment and ultrasonic-assisted enzymatic hydrolysis, Int. J. Food Sci. Technol. 49 (2014) 1932–1938, https://doi.org/10.1111/ijfs.12551.
[31] Z. Zhu, W. Zhu, J. Yi, N. Liu, Y. Cao, J. Lu, E.A. Decker, D.J. McClements, Effects of sonication on the physicochemical and functional properties of walnut protein isolate, Food Res. Int. 106 (2018) 853–861, https://doi.org/10.1016/j.foodres.2018.01.060.
[32] B. Nazari, M.A. Mohammadifar, S. Shojaee-Aliabadi, E. Feizollahi, L. Mirmoghtadaie, Effect of ultrasound treatments on functional properties and structure of millet protein concentrate, Ultrason. Sonochem. 41 (2018) 382–388, https://doi.org/10.1016/j.ultsonch.2017.10.002.
[33] X. Yang, Y.L. Li, S.Y. Li, A.O. Oladejo, Y.C. Wang, S.F. Huang, C.S. Zhou, X.F. Ye, H. L. Ma, Y.Q. Duan, Effects of ultrasound-assisted alpha-amylase degradation treatment with multiple modes on the extraction of rice protein, Ultrason. Sonochem. 40 (2018) 890–899, https://doi.org/10.1016/j.ultsonch.2017.08.028.
[34] H. Hu, J.H. Wu, E.C.Y. Li-Chan, L. Zhu, F. Zhang, X.Y. Xu, G. Fan, L.F. Wang, X. J. Huang, S.Y. Pan, Effects of ultrasound on structural and physical properties of soy protein isolate (SPI) dispersions, Food Hydrocolloids 30 (2013) 647–655, https://doi.org/10.1016/j.foodhyd.2012.08.001.
[35] Y. Zhang, Y. Li, S. Li, H. Zhang, H. Ma, *In situ* monitoring of the effect of ultrasound on the sulfhydryl groups and disulfide bonds of wheat gluten, Molecules 23 (2018) 1376, https://doi.org/10.3390/molecules23061376.
[36] J. Chandrapala, B. Zisu, M. Palmer, S. Kentish, M. Ashokkumar, Effects of ultrasound on the thermal and structural characteristics of proteins in reconstituted whey protein concentrate, Ultrason. Sonochem. 18 (2011) 951–957, https://doi.org/10.1016/j.ultsonch.2010.12.016.
[37] J.A. Resendiz-Vazquez, J.A. Ulloa, J.E. Urias-Silvas, P.U. Bautista-Rosales, J. C. Ramirez-Ramirez, P. Rosas-Ulloa, L. Gonzalez-Torres, Effect of high-intensity ultrasound on the technofunctional properties and structure of jackfruit

(Artocarpus heterophyllus) seed protein isolate, Ultrason. Sonochem. 37 (2017) 436–444, https://doi.org/10.1016/j.ultsonch.2017.01.042.

[38] Y. Zhang, B. Wang, C. Zhou, G.G. Atungulu, K. Xu, H. Ma, X. Ye, M. A. Abdualrahman, Surface topography, nano-mechanics and secondary structure of wheat gluten pretreated by alternate dual-frequency ultrasound and the correlation to enzymolysis, Ultrason. Sonochem. 31 (2016) 267–275, https://doi.org/10.1016/j.ultsonch.2015.11.010.

[39] L. Luo, Y. Zhang, K. Wang, H. Ma, M. Dong, *In situ* and real-time monitoring of an ultrasonic-assisted enzymatic hydrolysis process of corn gluten meal by a miniature near infrared spectrometer, Anal. Meth. 9 (2017) 3795–3803, https://doi.org/10.1039/c7ay00887b.